



Cite this: *Phys. Chem. Chem. Phys.*,
2016, **18**, 15046

A tryptophan-containing fluorescent intramolecular complex as a designer peptidic proton sensor†

V. Haridas,* Anita Yadav, Sakshi Sharma and Siddharth Pandey*

Received 22nd March 2016,
Accepted 4th May 2016

DOI: 10.1039/c6cp01912a

www.rsc.org/pccp

Pyrene and tryptophan groups judiciously placed on a novel molecular scaffold, namely, bispidine exhibited fluorescence due to the formation of an unprecedented emissive intramolecular complex in polar solvents. Upon protonation, the emission signal from the pyrene unit enhances at the expense of the emission signal from the complex. The probe demonstrates good sensitivity, excellent selectivity, and adequate reversibility towards proton sensing. The present design based on the bispidine scaffold opens up newer opportunities for the design of novel bispidine-peptide sensors.

Introduction

The design of stimuli-responsive molecules is an emerging theme as they can be transformed into smart materials and useful biochemical tools. Biology provides innumerable examples of molecular recognition of small molecules to even the size of protons with elegance, superiority and dexterity that are unmatched with any synthetic systems.¹ The majority of these feats in natural systems are accomplished by the amino acid side chain and their inbuilt chirality that provides a unique topology.² The design and development of sensitive and efficient proton sensing fluorescent probes are important as these designer probes can provide vital information about the chemical environment.^{3–6} Cellular pH plays a crucial role in biochemical events; hence protons are one of the most important targets. Fluorescence based techniques are powerful analytical methods for *in vivo* and *in vitro* sensing and imaging. The design and development of sensitive and efficient proton sensing fluorescent probes are important research topics, since these designer probes can provide vital information about the chemical environment.^{4–6} Combining fluorophores with peptides, nucleotides or polymers has considerably enhanced the performance of optical sensing systems. The proton “activatable probes” allow the researcher to control and manipulate fluorescence output signals by altering the chemical environment.⁷

In this paper, we report the design, synthesis and demonstration of a pyrene-based fluorescent intramolecular exciplex sensor for protons. We envisioned that positioning a fluorescent

amino acid proximal to another fluorophore is a simple strategy to spin out molecules with unique photophysical properties. We chose tryptophan (Trp), since it has an inherent fluorescence, and the choice of pyrene (Pyr) is primarily because it is well studied and has well separated excitation and emission wavelengths.⁸ These two fluorophores were combined with a rigid bicyclic scaffold, namely bispidine. Bispidine contains two piperidine rings in chair–chair conformation with nitrogens at a distance of ~2.9 Å. The chair–chair conformation with proximal nitrogen atoms makes bispidine architecturally an ideal framework to spatially display the attached fluorophores at close proximity. We functionalized one side of bispidine with Trp by an amide linkage, while Pyr was anchored to the other nitrogen through a methylene spacer. This design was envisaged by us since it allows the protonation of nitrogen on the side of Pyr while keeping the Trp-appended nitrogen unaffected thus leading to differences in the spectroscopic signatures.

Experimental

Synthesis of compounds 1–3

All reagents employed in the synthesis were used without further purification. All solvents were distilled or dried using an appropriate drying agent prior to use. Reactions were monitored by thin layer chromatography (TLC). Silica gel G (Merck) was used for TLC and column chromatography. The silica gel columns were generally made from the slurry in hexane, hexane/ethyl acetate or chloroform. The Fisher-Johns melting point apparatus was used for recording the melting point. IR spectra were recorded on a Nicolet, Protégé 460 spectrometer as KBr pellets. ¹H NMR spectra were recorded on a Bruker-DPX-300 (¹H, 300 MHz; ¹³C, 75 MHz) spectrometer

Department of Chemistry, Indian Institute of Technology Delhi, Hauz Khas,
New Delhi, 110016, India. E-mail: haridasv@chemistry.iitd.ac.in,
sipandey@chemistry.iitd.ac.in

† Electronic supplementary information (ESI) available. See DOI: 10.1039/c6cp01912a

using tetramethylsilane (^1H) as an internal standard. Coupling constants are in Hz and the ^1H NMR data are reported as s (singlet), d (doublet), br (broad), br d (broad doublet), t (triplet), q (quartet), and m (multiplet). HRMS were recorded using a AB Sciex, 1011273/A model by the ESI-technique.

Preparation of compound 3. To a well stirred and ice cooled solution of **3** (0.286 g, 0.91 mmol), in methanol (10 mL), were added 0.050 g of Pd/C and H_2 gas was purged for 4 hours. The progress of reaction was monitored by TLC. The reaction mixture was filtered through a sintered funnel and washed with methanol. Methanol was evaporated under reduced pressure to yield 0.205 g of the product Bisp NH (Boc) as yellow oil.

Yield: quantitative

To an ice-cooled solution of Bisp NH (Boc) (0.205 g, 0.91 mmol) in 60 mL of dry acetonitrile were added triethylamine (0.5 mL, 3.64 mmol) and $\text{Br}-\text{CH}_2-\text{CO}-\text{NH}-\text{CH}_2-\text{pyrene}$ (0.320 g, 0.91 mmol). The reaction mixture was left stirred overnight at room temperature. The reaction mixture was evaporated and dissolved in 80 mL of dichloromethane, washed with 2N H_2SO_4 , saturated aqueous NaHCO_3 solution and finally with water. The organic layer was dried over anhydrous Na_2SO_4 , filtered and evaporated to yield 0.300 g of the crude compound. Column chromatography over silica gel (100–200 EtOAc:hexane, 6:4) gave 0.250 g of the pure product **3**.

Preparation of compound 1. To a well stirred and ice cooled solution of **3** (0.100 g, 0.201 mmol), in dry CH_2Cl_2 (2 mL), was added TFA (0.4 mL, 4.83 mmol) and stirred at room temperature for 4 h. The reaction mixture was subjected to vacuum to remove CH_2Cl_2 and TFA to afford 80 mg of the product Bisp NH (pyrene) as yellow oil.

To an ice-cooled solution of Boc-Trp-OH (0.061 g, 0.201 mmol) in 80 mL of dry dichloromethane, were added *N*-hydroxy-succinimide (0.030 g, 0.241 mmol) and DCC (0.050 g, 0.241 mmol) and stirred for 10 min. Bisp NH (pyrene) (0.080 g, 0.201 mmol) and triethylamine (0.1 mL, 0.804 mmol) were added. The reaction mixture was stirred overnight, filtered and washed the filtrate with 2N H_2SO_4 , saturated aqueous NaHCO_3 solution and finally with water. The organic layer was dried over anhydrous Na_2SO_4 and evaporated to yield 0.100 g of crude compound. Column chromatography over silica gel (100–200 EtOAc:hexane, 8:2), gave 0.50 g of the pure product **1**.

Preparation of compound 2. To a well stirred and ice cooled solution of **3** (0.160 g, 0.322 mmol), in dry CH_2Cl_2 (2 mL), was added TFA (1 mL, 12.44 mmol) and stirred at RT for 4 h. The reaction mixture was subjected to vacuum to remove CH_2Cl_2 and TFA to afford 128 mg of the product Bisp NH (pyrene) as yellow oil.

To an ice-cooled solution of Boc-Leu-OH (0.074 g, 0.322 mmol) in 80 mL of dry dichloromethane, were added *N*-hydroxy-succinimide (0.050 g, 0.386 mmol) and DCC (0.080 g, 0.386 mmol) and stirred for 10 min. Bisp NH (pyrene) (0.128 g, 0.322 mmol) and triethylamine (0.2 mL, 1.74 mmol) were added. The reaction mixture was stirred overnight and filtered, and the filtrate was washed with 2N H_2SO_4 , saturated aqueous NaHCO_3 solution and finally with water. The organic layer was dried over anhydrous

Na_2SO_4 and evaporated to yield 0.180 g of crude compound. Column chromatography over silica gel (100–200 EtOAc:hexane, 6:4), gave 0.100 g of the pure product **2**.

Materials

The following solvents were used as received: 2,2,2-trifluoro-ethanol (extra pure, 99.8%, Acros Organics), acetonitrile (LC-MS Chromasolv, $\geq 99.9\%$, Sigma-Aldrich), chloroform (ACS spectrophotometric grade, $\geq 99.8\%$, Sigma-Aldrich), propylene carbonate (Chromasolv for HPLC, 99.7%, Sigma-Aldrich), *N,N*-dimethylformamide (Chromasolv plus for HPLC, $\geq 99.9\%$, Sigma-Aldrich), acetone (Chromasolv for HPLC, $\geq 99.9\%$, Sigma-Aldrich), dimethylsulfoxide (Chromasolv plus for HPLC, $\geq 99.9\%$, Sigma-Aldrich), ethylene glycol (spectrophotometric grade, $\geq 99\%$, Sigma-Aldrich), ethylacetate (HPLC, 99.8%, Spectrochem), tetrahydrofuran (Lichrosolv chromatography for HPLC, 99.7%, Merck) and ethanol (99.9%, Merck). The following salts are used: cobalt chloride (98%, Qualigens), sodium chloride (99.9%, Qualigens), potassium chloride (99.8%, Qualigens), ammonium chloride (99.8%, Qualigens), cesium chloride (99.8%, Qualigens), calcium chloride (98%, Merck) and copper(II) sulfate 5-hydrate (99%, Merck). Sodium hydroxide (98%) and nitric acid (ACS, 69%), were purchased from Fischer scientific and Merck, respectively. Proton sensing experiments were carried out by simple addition of conc. nitric acid to the solution.

Methods

The stock solutions of compounds **1**, **2**, and **3** were prepared in ethanol and stored in an amber glass vial at 4 ± 1 °C. The required amounts of compounds **1**, **2**, and **3** to prepare stock solutions were weighed using a Denver Instrument balance having a precision of ± 0.1 mg. An appropriate amount of solutions of compounds **1**, **2**, and **3** from the stock was transferred to the 1 cm² quartz cuvette. Ethanol was evaporated under a gentle stream of high purity nitrogen gas.

A Perkin-Elmer Lambda 35 double beam spectrophotometer with variable bandwidth and a Peltier-temperature controller was used for acquisition of the UV-vis molecular absorbance data. Steady-state emission and excitation spectra were acquired on a model FL 3-11, Fluorolog-3 modular spectrofluorimeter with single Czerny–Turner grating excitation and emission monochromators having a 450W Xe arc lamp as the excitation source and a PMT as the detector. This spectrofluorimeter was purchased from Horiba-Jobin Yvon, Inc. The temperature was controlled using a Thermo NESLAB RTE7 circulating chiller bath having a stability of ± 0.01 °C. Since the use of pyrene and pyrene-appended compounds is usually known to result in high fluorescence quantum yields,⁹ the blank signal was $< 0.1\%$ of the sample signal in all cases. This is also considered to be a necessary condition for fluorescence lifetime measurements.¹⁰ All absorbance and fluorescence data were acquired using 1 cm² quartz cuvettes. Spectral response from appropriate blanks was subtracted before data analysis. The time-resolved fluorescence measurements were carried out using a Horiba-Jobin Yvon Fluorocube time-correlated single photon counting (TCSPC)

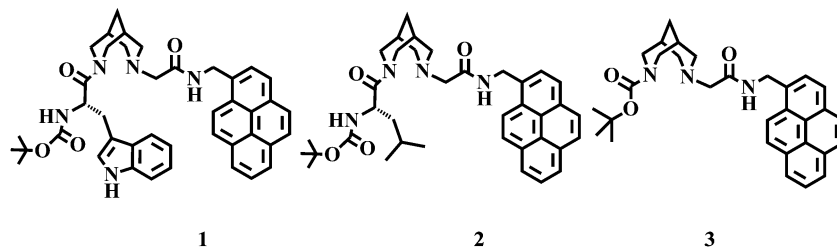


Fig. 1 Structures of the bispidine-based compounds.

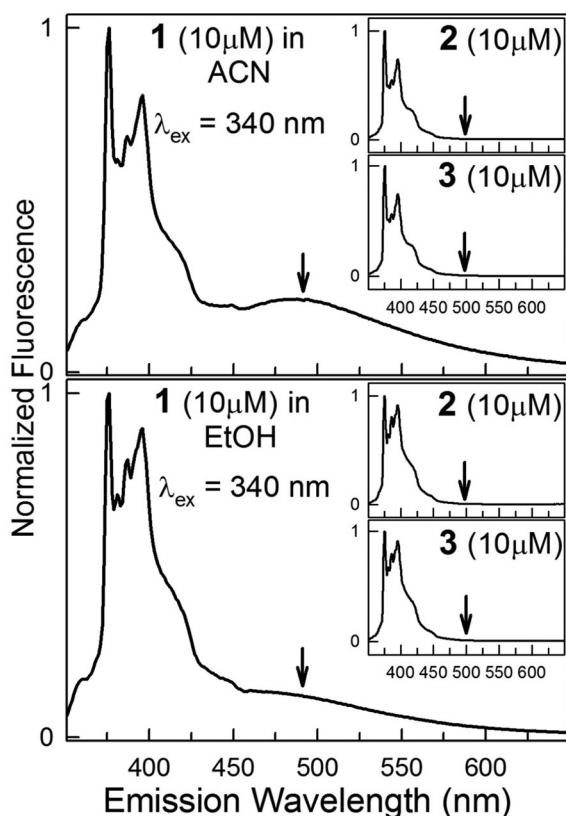


Fig. 2 Normalized fluorescence emission spectra of **1** at 25 °C. Emission spectra of controls **2** and **3** under identical conditions are shown in insets. Arrows highlight the presence and absence of the emission band corresponding to the intramolecular complex in **1** and **2/3**, respectively.

intramolecular in nature, the fluorescence spectra of **1** are acquired at five different concentrations in the range 1–50 μM in ethanol under ambient conditions. The results presented in Fig. S3 (ESI[†]) reveal the normalized fluorescence spectra of **1** to be independent of the concentration of the compound; the normalized fluorescence scans at five different concentrations of **1** overlap with no statistical differences. This implies the complex formation to be intramolecular in nature.

In order to decipher the role of the Trp unit on the molecular scaffold to form this fluorescent complex, emission spectra from two control compounds, **2** and **3** (Fig. 1), were acquired under identical conditions. Contrary to that observed for **1**, no low-energy structureless fluorescence is observed for any of the control compounds in ACN and EtOH, respectively (Fig. 2). It is

Table 1 Ratio of the emission intensity of complex (475 nm)-to-pyrene band I (376 nm) for **1** in different solvents at 25 °C

Solvent	$I_{\text{Complex}}/I_{\text{PyrI}} (\times 10^{-2})$
Polar-aprotic	
Acetonitrile	18.6 ± 0.6
Acetone	12.2 ± 0.5
Ethylacetate	10.4 ± 0.3
Propylene carbonate	8.7 ± 0.3
Tetrahydrofuran	8.2 ± 0.3
Dimethylformamide	6.3 ± 0.2
Dimethyl sulfoxide	4.6 ± 0.2
Polar-protic	
2,2,2-Trifluoroethanol	21.6 ± 0.6
Ethanol	15.5 ± 0.5
Ethylene glycol	3.7 ± 0.1
Chlorinated	
Dichloromethane	17.5 ± 0.5
Chloroform	10.7 ± 0.3

clear that the indole unit must be present to observe this intramolecular fluorescent complex. Apart from ACN and EtOH, the low-energy structureless broad emission band also appears when **1** is dissolved in several other protic, aprotic, and chlorinated polar solvents (Fig. S4, ESI[†]). However, an estimation of the complex-to-pyrene band I fluorescence intensity ratio ($I_{\text{Complex}}/I_{\text{PyrI}}$ representing $I_{475\text{nm}}/I_{376\text{nm}}$, listed in Table 1) reveals that this intramolecular fluorescent complex formation depends on the viscosity of the solvent; fluorescence from the complex is less in more viscous solvents.

It is noted that when the electron/charge donor and acceptor form part of the same molecule, intramolecular charge-transfer states leading to detectable fluorescence are sometimes termed “exciplex” states.^{16–20} In the case of intramolecular donor-acceptor systems with a flexible linkage, the conformations having face-to-face geometry were initially termed “exciplex conformations”. However, in a seminal work it was shown that a sandwich conformation was not a prerequisite for fluorescence in such systems.²¹ Along with structural and geometrical factors a medium effect is also known to contribute to the thermodynamics and the kinetics of the intramolecular charge transfer process.²² Rapid photoinduced long-range electron transfer followed by emissive charge recombination was earlier demonstrated for the donor-acceptor systems with rigidly extended bridges.^{23,24} It was recognized that the steric requirements were perhaps not so restrictive in forming polar exciplexes; the appearance of exciplex fluorescence is hypothesized to be due

to conformationally close chromophores. We believe that in our case the conformational proximity between donor Trp and excited-state acceptor Pyr results in the formation of an intramolecular fluorescent complex.

We explored the effect of dissolved O₂ on the fluorescence emission from the complex. In EtOH, for $\lambda_{\text{ex}} = 265$ nm, the $I_{\text{Complex}}/I_{\text{PyrI}}$ values are 0.16(± 0.01) and 0.15(± 0.01) for the unpurged and purged samples, respectively (purged samples are the ones where most of the dissolved O₂ is expelled by 30 min of gentle purging with the highest purity Ar gas, Fig. S5, ESI†). It is clear that quenching of the fluorescence of the Pyr unit and that of the emissive complex by molecular oxygen, a ubiquitous quencher, are fairly similar.^{25,26} This renders the evaluation of this fluorescent complex for sensing and other applications a favourable simplicity.

Time-resolved fluorescence was employed to obtain insights into this unprecedented fluorescent complex formation involving the Trp unit. Excited-state emission intensity decay data were collected for **1** along with controls **2** and **3** in ACN and EtOH, respectively. For both the control compounds intensity decay at 376 nm (Pyr group emission) fit best to a single-exponential decay model (Table 2) further confirming the absence of the fluorescent complex for these two control compounds. For **1** in ACN, the intensity decay at 480 nm (corresponding to the complex) best fits to a double exponential decay model though the fit to a single exponential decay model is not too inadequate (Fig. 3). This may imply the presence of two excited-state species for **1** – one corresponding to the uncomplexed and the other to the stable complex. However, a careful examination of the data presented in Table 2 reveals that the two pre-exponential factors obtained from the fit are not equal to each other in magnitude and opposite in sign. If the complex is only formed after the excitation of **1**, the two pre-exponential factors should be equal in magnitude and opposite in sign.²⁷ However, in case the rate constant of the complex formation in the excited-state is too large (*i.e.*, the complex formation is faster than the time-resolution of the instrument) and/or some population of the complex is present in the ground

state, then equal and opposite pre-exponential factors may not be recovered as a result of the fitting protocol. Based on the fact that the fit of the intensity decay at 480 nm using a single exponential is not too inadequate (and the absence of the ground-state complex in the absorbance spectral data, *vide supra*), we lean toward the possibility of rapid formation of the complex in the excited-state. The fit of the intensity decay at 376 nm (corresponding to the Pyr unit) for **1** in ACN to a single exponential decay model is clearly unacceptable; the use of a two-exponential decay model results in considerably improved fitting (Fig. 3 and Table S1, ESI†). Apart from supporting the presence of two excited species, this also implies measurable dissociation of the excited complex back to the excited uncomplexed species. The similarities in the two recovered decay times at 376 nm and at 480 nm, respectively, along with the presence of –ve pre-exponential factors (in excited complex decay) further emphasize the existence and formation of complexes in the excited state (Table 2).

The intensity decay data of **1** in EtOH are more complicated. The decay at 480 nm requires three exponentials (not only the reduced χ^2 is improved substantially from the 2- to the 3-exponential function, the two recovered decay times for the 2-exponential model are fairly similar and hence unacceptable, Fig. S6 and Table S1, ESI†). The decay at 376 nm also fits better to a 3-exponential model with similarities in the three recovered decay times at 376 nm and at 480 nm, respectively. This emphasizes the presence of three excited state species, where the additional species could be the ground-state complex exhibiting a different decay time. Alternatively, the polar-protic media on occasions introduces an additional decay component due to the presence of H-bonded species in the excited-state.^{28–31}

The usefulness of the fluorescent complex formed by **1** is amply demonstrated *via* the change in its signal in the presence of H⁺. The emission of **1** is found to have high sensitivity, excellent selectivity, and good reversibility to H⁺ in both ACN and EtOH. As the H⁺ is added incrementally, the fluorescence signal of the complex diminishes and that of the Pyr unit augments resulting in a significant decrease in $I_{\text{Complex}}/I_{\text{PyrI}}$ (Fig. 4). The clear appearance of an isoemissive point at ~ 453 nm is an indication that the complex is converted back to the uncomplexed conformer by H⁺ in a reversible manner. As compared to EtOH, the sensitivity to H⁺ in polar-aprotic ACN is higher (for [H⁺] = 10^{–5} M, the decrease in $I_{\text{Complex}}/I_{\text{PyrI}}$ is $\sim 78\%$ in ACN *versus* $\sim 18\%$ in EtOH, Fig. S7, ESI†). The decrease in $I_{\text{Complex}}/I_{\text{PyrI}}$ is fairly linear till [H⁺] = 10^{–5} M [for ACN, $R^2 = 0.973$ with slope $\approx -2.1(\pm 0.1) \times 10^4 \text{ M}^{-1}$ and for EtOH, $R^2 = 0.990$ with slope $\approx -4.5(\pm 0.2) \times 10^3 \text{ M}^{-1}$]. While within ACN, the plateau in $I_{\text{Complex}}/I_{\text{PyrI}}$ is reached for [H⁺] > 10^{–5} M, in EtOH it is reached for a fold higher [H⁺] of 10^{–4} M (Fig. S7, ESI†).

Intensity decay data of **1** collected at 376 nm and 480 nm, respectively, in the presence of sufficiently high [H⁺] (=3.16 $\times 10^{-3}$ M, where $I_{\text{PyrI}}/I_{\text{Complex}}$ attains a plateau) afford insight into the possible mode of H⁺ recognition. In ACN, in the presence of [H⁺], the intensity decay at 376 nm and that at 480 nm again fit best to a double-exponential decay model with recovered decay times similar to those extracted when no [H⁺] was present (Table 2 and Table S1, ESI†). However, for the decay at

Table 2 Recovered intensity decay parameters for **1**, **2** and **3** at 25 °C. Excitation was carried out using a 340 nm LED. Errors associated with decay times and pre-exponential factors are $\leq \pm 5\%$

Compound	λ_{em} (nm)	τ_1 (ns)	τ_2 (ns)	τ_3 (ns)	α_1	α_2	α_3	χ^2
Acetonitrile								
1	376	1.8	12.6		0.86	0.14		1.13
	480	3.7	11.9		–0.13	0.87		1.08
1 + 3.16 $\times 10^{-3}$ M [H ⁺]	376	1.7	14.6		0.40	0.60		1.59
	480	1.8	12.8		0.72	0.28		1.34
2	376	17.2			1.00			1.56
3	376	17.5			1.00			1.41
Ethanol								
1	376	1.0	6.2	18.3	0.49	0.31	0.19	1.34
	480	0.8	8.1	15.9	0.26	–0.24	0.49	1.18
1 + 3.16 $\times 10^{-3}$ M [H ⁺]	376	1.2	6.5	26.7	0.51	0.11	0.38	1.06
	480	1.0	5.1	23.1	0.55	0.27	0.19	1.03
2	376	22.5			1.00			1.15
3	376	23.6			1.00			2.15

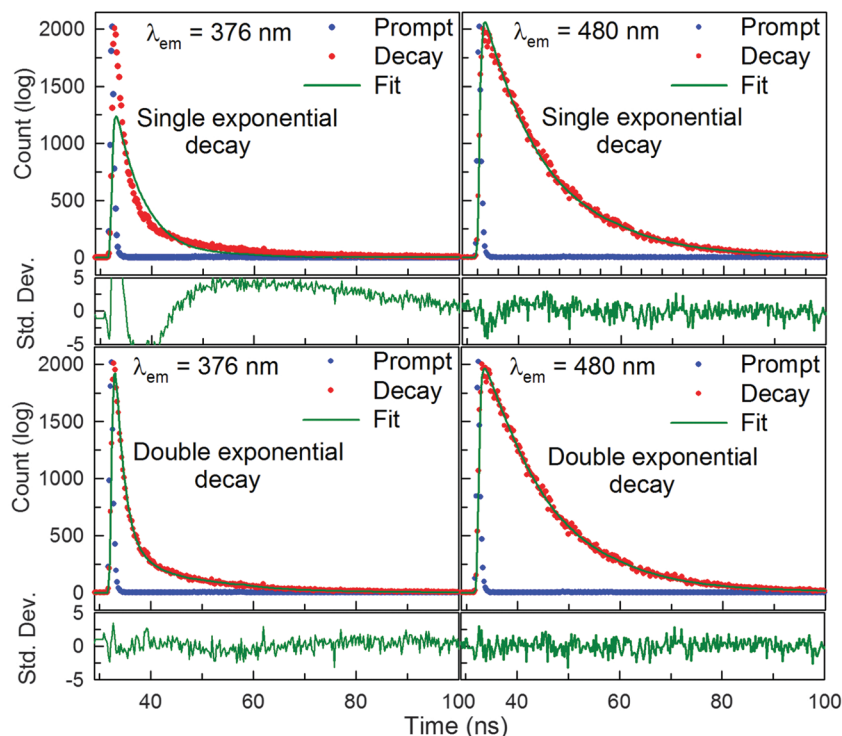


Fig. 3 Fit of excited-state intensity decay data of **1** in ACN at 25 °C. Residuals are provided below each panel. The top two panels show fits of the decays at 376 nm and 480 nm, respectively, to a single exponential decay model, whereas the two lower panels show the fits of the same decays to the double exponential decay model.

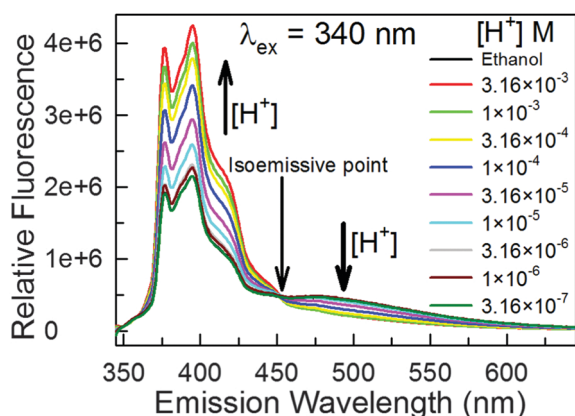
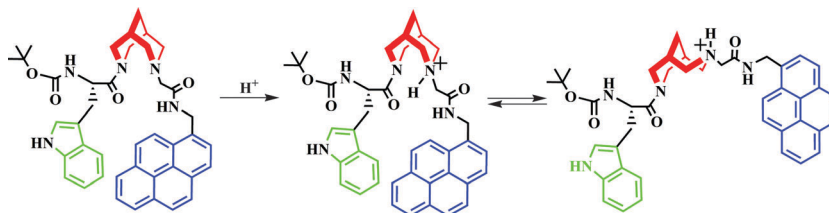


Fig. 4 Fluorescence emission spectra of **1** (10 μM) in EtOH in the presence of varying $[H^+]$ at 25 °C.

376 nm, the pre-exponential factors are very different in the absence and the presence of H^+ implying the differential distribution of the species due to their H^+ -induced interconversion. Interestingly, the $-ve$ pre-exponential factor recovered in the decay at 480 nm in the absence of $[H^+]$ highlighting the formation of the complex in the excited-state (*vide supra*) is no longer observed as both the pre-exponential factors in the presence of $[H^+]$ are $+ve$ (Table 2). This indicates that $[H^+]$ has hindered the formation of the fluorescent complex possibly by protonating the Pyr-attached bispidine nitrogen. Decay parameters recovered in the presence of $[H^+]$ for **1** in EtOH show similar trends as those in ACN and thus support this proposition (Table 2). We believe that the protonation at the Pyr side of bispidine nitrogen changes the conformation of **1** from chair-chair to boat-chair hence rendering it unsuitable for intramolecular complex formation (Scheme 2).³² The fact that **1** is stable in the presence of $3.16 \times 10^{-3} M [H^+]$ is amply evident by the mass spectroscopic data (Fig. S8, ESI[†]).



Scheme 2 Schematic representation of the proposed protonation induced conformational change.

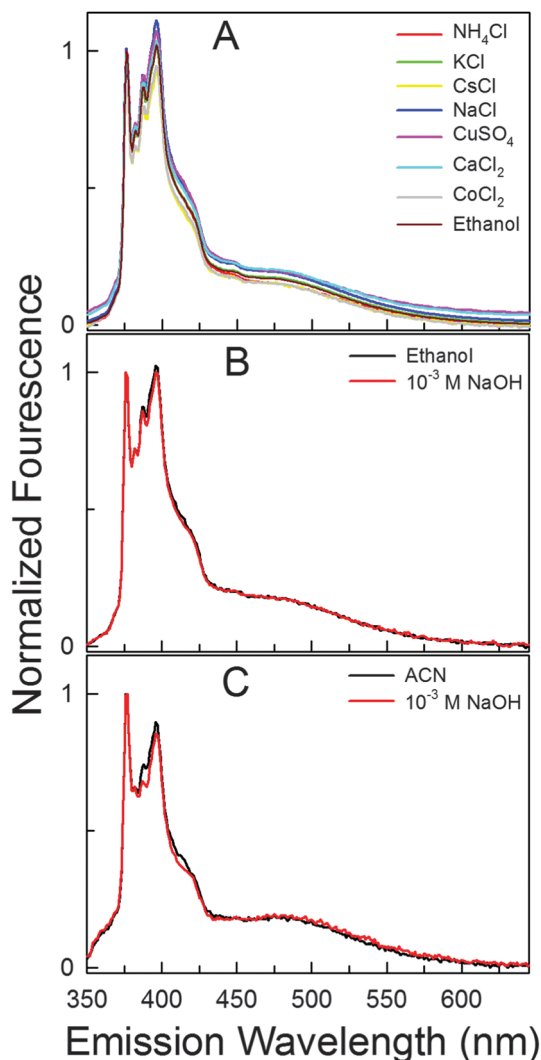


Fig. 5 Normalized fluorescence emission spectra ($\lambda_{\text{ex}} = 340 \text{ nm}$) of **1** ($10 \mu\text{M}$) (A) in the presence of various salts (0.01 M) in ethanol at 25°C (A), in the presence of 10^{-3} M NaOH in ethanol (B), and in ACN (C).

The excellent selectivity for H^+ recognition by **1** is exhibited by the fact that no change in the fluorescence signal is observed even in the presence of as high as 0.01 M NH_4^+ , K^+ , Na^+ , Cu^{2+} , Ca^{2+} , Co^{2+} , and Cs^+ , respectively (Fig. 5). It is noteworthy that addition of 10^{-3} M NaOH to **1** in ACN as well as in EtOH also results in no change in the fluorescence from the complex. Sensitive and selective fluorescence-based recognition of H^+ by **1** is also accompanied by good reversibility. The $I_{\text{Complex}}/I_{\text{Pyri}}$ decreased as a result of $[\text{H}^+]$ addition and it is readily recovered back upon addition of equal $[\text{OH}^-]$ (Fig. 6). For subsequent cycles also, the decrease and recovery of the signal may be considered adequate.

Conclusions

In summary, we have presented bispidine as a promising scaffold for the sensing of H^+ based on fluorescence. The designer system described showed an unusual and unique ability to sense H^+

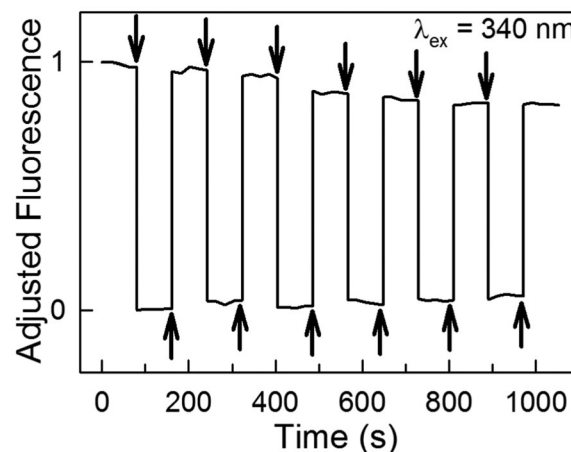


Fig. 6 Adjusted fluorescence of **1** ($10 \mu\text{M}$) in ethanol (1 and 0 depict maximum and minimum of $I_{\text{Complex}}/I_{\text{Pyri}}$ in the absence and presence of $3.16 \times 10^{-3} \text{ M}$ $[\text{H}^+]$ for the first addition, respectively), as a function of scanning time. Downward arrows indicate addition of $3.16 \times 10^{-3} \text{ M}$ $[\text{H}^+]$ and upward arrows depict the addition of $3.16 \times 10^{-3} \text{ M}$ $[\text{OH}^-]$. Additions of $[\text{H}^+]$ and $[\text{OH}^-]$ are carried out sequentially.

through intramolecular fluorescent complex formation. The concept was demonstrated by appending a biologically relevant unit such as Trp in the design, which gives rise to the formation of an unprecedented fluorescent intramolecular complex with pyrene. The potential of the bispidine framework to exist in chair-chair, boat-chair, chair-boat, and boat-boat conformations can expand further the scope of the design.

Acknowledgements

This work was generously funded by a grant to S. P. from DST-SERB, GoI [grant no. SB/S1/PC-80/2012]. A. Y. thanks CSIR, GoI and S. S. thanks UGC, GoI for their fellowships. The authors would like to thank DST-FIST for the instrument grant for the mass spectrometer.

Notes and references

- M.-G. Ludwig, M. Vanek, D. Guerini, J. A. Gasser, C. E. Jones, U. Junker, H. Hofstetter, R. M. Wolf and K. Seuwen, *Nature*, 2003, **425**, 93–98.
- F. Galindo, M. I. Burguete, L. Vigarà, S. V. Luis, N. Kabir, J. Gavrilovic and D. A. Russell, *Angew. Chem., Int. Ed.*, 2005, **44**, 6504–6508.
- (a) J. Han, A. Loudet, R. Barhoumi, R. C. Burghardt and K. A. Burgess, *J. Am. Chem. Soc.*, 2009, **131**, 1642–1643; (b) H. F. Higginbotham, R. P. Cox, S. Sandanayake, B. A. Graystone, S. J. Langford and T. D. M. Bell, *Chem. Commun.*, 2013, **49**, 5061–5063.
- D. Staneva, M. S. I. Makki, T. R. Sobahi, P. Bosch, R. M. Abdel-Rahman, A. Asiri and I. Grabchev, *J. Lumin.*, 2015, **162**, 149–154.
- G. R. C. Hamilton, S. K. Sahoo, S. Kamila, N. Singh, N. Kaur, B. W. Hyland and J. F. Callan, *Chem. Soc. Rev.*, 2015, **44**, 4415–4432.

- 6 B. He, J. Dai, D. Zherebetsky, T. L. Chen, B. A. Zhang, S. J. Teat, Q. Zhang, L. Wang and Y. Liu, *Chem. Sci.*, 2015, **6**, 3180–3186.
- 7 S. Lee, K. Park, K. Kim, K. Choi and I. C. Kwon, *Chem. Commun.*, 2008, 4250–4260.
- 8 F. M. Winnik, *Chem. Rev.*, 1993, **93**, 587–614.
- 9 J. B. Birks, *Photophysics of Aromatic Molecules*, John Wiley & Sons, London, 1970.
- 10 G. A. Baker, S. Pandey and F. V. Bright, *Appl. Spectrosc.*, 1999, **53**, 1475–1479.
- 11 V. Haridas, S. Sadanandam, M. V. S. Gopalakrishna, M. B. Bijesh, R. P. Verma, S. Chinthalapalli and A. Shandihya, *Chem. Commun.*, 2013, **49**, 10980–10982.
- 12 E. Gudgn, R. Lopez-Deigado and W. R. Ware, *J. Phys. Chem.*, 1983, **87**, 1559–1565.
- 13 D. C. Dong and M. A. Winnik, *Can. J. Chem.*, 1984, **62**, 2560–2565.
- 14 D. S. Karpovich and G. J. Blanchard, *J. Phys. Chem.*, 1995, **99**, 3951–3958.
- 15 W. E. Acree, Jr., S. A. Tucker and D. C. Wilkins, *J. Phys. Chem.*, 1993, **97**, 11199–11203.
- 16 H. Oevering, M. N. Paddon-Row, M. Heppener, A. M. Oliver, E. Cotsaris, J. W. Verhoeven and N. S. Hush, *J. Am. Chem. Soc.*, 1987, **109**, 3258–3269.
- 17 M. R. Wasielewski, *Chem. Rev.*, 1992, **92**, 435–461.
- 18 D. Gust, T. A. Moore and A. L. Moore, *Acc. Chem. Res.*, 1993, **26**, 198–205.
- 19 J. P. Sauvage, J. P. Collin, J. C. Chambron, S. Guillerez, C. Coudret, V. Baltani, F. Barigelletti, L. De Cola and L. Flamigni, *Chem. Rev.*, 1994, **94**, 993–1019.
- 20 A. Osuka, S. Marumo, N. Mataga, S. Taniguchi, T. Okada, I. Yamazaki, Y. Nishimura, T. Ohno and K. Nozaki, *J. Am. Chem. Soc.*, 1996, **118**, 155–168.
- 21 T. Scherer, I. H. M. Van Stokkum, A. M. Brouwer and J. W. Verhoeven, *J. Phys. Chem.*, 1994, **98**, 10539–10549.
- 22 P. Pasman, G. F. Mes, N. W. Koper and J. W. Verhoeven, *J. Am. Chem. Soc.*, 1985, **107**, 5839–5843.
- 23 J. Jortner, M. Bixon, B. Wegewijs, J. W. Verhoeven and R. P. H. Rettschnick, *Chem. Phys. Lett.*, 1993, **205**, 451–455.
- 24 B. Wegewijs, A. K. F. Ng, R. P. H. Rettschnick and J. W. Verhoeven, *Chem. Phys. Lett.*, 1992, **200**, 357–363.
- 25 B. Valeur and M. N. Berberan-Santos, *Molecular Fluorescence: Principles and Applications*, Wiley-VCH, Weinheim, 2nd edn, ch. 6, 2012.
- 26 J. R. Lakowicz, *Principles of Fluorescence Spectroscopy*, Kluwer Academics/Plenum Publishers, New York, 3rd edn, ch. 8, 2006.
- 27 J. B. Birks, *Rep. Prog. Phys.*, 1975, **38**, 903–974.
- 28 V. Ramamurthy and K. S. Schanze, *Organic Molecular photochemistry*, Marcel Dekker, Inc., New York, 1999.
- 29 K. L. Han and G. J. Zhao, in *Hydrogen Bonding and Transfer in the Excited State*, ed. K. L. Han and G. J. Zhao, J. Wiley & Sons, 2010.
- 30 J. P. Bridhkoti, H. Mishra, H. C. Joshi and S. Pant, *Spectrochim. Acta, Part A*, 2011, **79**, 412–417.
- 31 M. J'ozefowicza, J. R. Heldta, J. Karolczakb and J. Heldta, *Z. Naturforsch.*, 2003, **58a**, 144–156.
- 32 S. Norrehed, M. Erdelyi, M. E. Light and A. Gogoll, *Org. Biomol. Chem.*, 2013, **11**, 6292–6299.